INTERNATIONAL JOURNAL OF CIRCUITS, SYSTEMS AND SIGNAL PROCESSING
DOI: 10.46300/9106.2020.14.56 Volume 14, 2020

Retinal Image Enhancement using Ordering Gap Adjustment and Brightness Specification

P. Vonghirandecha, S. Kansomkeat, and S. Intajag

Received: May 15, 2020. Revised: July 17, 2020. Accepted: July 27, 2020. Published: July 29, 2020.

***Abstract*—**Color retinal image enhancement plays an important role in improving an image quality suited for reliable diagnosis. For this problem domain, a simple and effective algorithm for image contrast and color balance enhancement namely Ordering Gap Adjustment and Brightness Specification (OGABS) was proposed. The OGABS algorithm first constructs a specified histogram by adjusting the gap of the input image histogram ordering by its probability density function under gap limiter and Hubbard's dynamic range specifications. Then, the specified histograms are targets to redistribute the intensity values of the input image based on histogram matching. Finally, color balance is improved by specifying the image brightness based on Hubbard's brightness specification. The OGABS algorithm is implemented by the MATLAB program and the performance of our algorithm has been evaluated against data from STARE and DiaretDB0 datasets. The results obtained show that our algorithm enhances the image contrast and creates a good color balance in a pleasing natural appearance with a standard color of lesions.

***Keywords*—**Retinal images, gap adjustment, brightness specification, image contrast and color balance enhancement, histogram matching.

I. INTRODUCTION

ACCORDING to the World Health Organization, Age Related Macular Degeneration (AMD) is the third cause of blindness after cataract and glaucoma in the elderly worldwide [1] [2]. Most currently validated AMD evaluation systems are based on a retinal color photography. However, these images may be unsatisfactory for diagnosis due to their low quality; especially from tone resolution caused by camera properties and the experience of photographers [3] [4] [5]. Such images need to be enhanced to provide better visibility of the retinal anatomical structures.

Histogram equalization (HE) is a common contrast enhancement technique which uses the cumulative distribution function (CDF) of the input image for stretching its dynamic range of the gray-levels. The main drawback of HE is that it tends to shift the mean intensity values to the middle of the dynamic range and result in over-enhancement or unnatural appearances. To overcome the described problems, various method including BPHEME [6], BPDHE [7], BPDFHE [8] have been proposed for brightness preservation. However, those algorithms are not appropriate when the input image is underexposed or overexposed; because, they provide output images with a mean brightness close to the input and are therefore unsuitable for human perception.

An image enhancement based on luminosity and contrast adjustment (LCA) [9], which augments HE, has been designed for a color retinal image. LCA creates luminance gain matrix by correcting the gamma of the value channel, V, in hue-saturation-value (HSV) color space, and uses it to enhance the intensity values in red(R), green(G), and blue(B) channels. The image contrast was improved by enhancing the luminosity channel, L, in L*a*b* color space by applying the CLAHE [10] with the number of tiles and clip limit equal to 8×8 pixels and 0.01, respectively. LCA could handle contrast enhancement, but does not consider color balance.

Recently, an automatic screening and grading (ASG) of AMD [11] has been proposed to classify AMD in a telemedicine context. In this method, a square region of interest (ROI) of retinal image was selected from the whole image. Next, a median filter with a kernel size of one-fourth of the ROI size was applied to the green channel for estimating the background illumination. The obtained filtered image was then subtracted from the original green channel. Finally, the green values were multiplied by 2 for contrast improvement and shifted by the mean value of their intensity range for visualization purposes.

Motivated and inspired by the findings published in [12], Hubbard *et al.* analyzed brightness, contrast, and color balance of digital compared with film retinal images in the Age-Related Eye Disease Study (AREDS) for AMD screening. They divide 256 intensity levels into 16 scales, and define the brightness at the peaks of each color channel to 12/16, 6/16, and 2/16 for R, G, and B, respectively, resulting in the color balance is yielded at the band ratios G/R = 0.5 and B/R = 0.17. The modeled contrast is spanned in the ranges [7/16, 15/16] for R, [1/16, 9/16] for G, and [1/16, 3/16] for B channels.

We propose an improvement to previously existing algorithms in order to allow physicians to more easily and accurately diagnose the retinal diseases. The purpose of this improvement, and the main contribution of our work, is to provide a good quality fundus image with a standard color of

P. Vonghirandecha is with the Department of Computer Science, Faculty of Science, Prince of Songkla University, Songkhla, Thailand.
(e-mail: preecha.v@psu.ac.th).
S. Kansomkeat is with the Department of Computer Science, Faculty of Science, Prince of Songkla University, Songkhla, Thailand.
(e-mail: supaporn.k@psu.ac.th).
S. Intajag is with the Department of Computer Science, Faculty of Science, Prince of Songkla University, Songkhla, Thailand.
(e-mail: sathit.i@psu.ac.th).

the AMD lesions and more easily visible the anatomical details.

The performance of our method was evaluated using two publicly available datasets, Structured Analysis of the Retina (STARE) [13] and the Diabetic Retinopathy Database (DiaretDB0) [14]. The STARE dataset, acquired by Hoover *et al*. [13], consists of 32 images. The images were taken with a 35° field of view (FOV), and each occupies, and 700×605 pixels, and is stored in 24-bit PPM format. The DiaretDB0 dataset, acquired by Kauppi *et al*. [14], consists of 20 normal images and 110 containing signs of diabetic retinopathy. The images were taken with a 50° FOV, are 1500×1152 pixels large, and stored in 24-bit PNG format. Both PPM and PNG formats occur uncompressed and with lossless data compression respectively. Both datasets have different factors of FOV and image sizes; however, our method could handle these factors as seen in the experimentations.

The paper proceeds as follows: the proposed method is described in detail in Section II. Our experimental results appear in Section III, and conclusions in section IV.

II. THE PROPOSED ALGORITHM

The method of Hubbard *et al*. [12] used Photoshop to improve the color retinal images within ROI. Their ROI does not include the optic disk but focus at the macular area. The color data in ROI are adjusted and specified by their color model. The proposed method uses Hubbard's color model to improve the image quality by designing OGABS (Ordering Gap Adjustment and Brightness Specification) algorithm, which could automatically enhance the image with the MATLAB program.

To increase the visibility of the anatomical details with standard color of lesions, we propose OGABS for effectively improving contrast and color balance based on Hubbard's specification model. OGABS consists of three modules (see Fig. 1): i) *specified histogram* under gap limiter and Hubbard's dynamic range specifications. ii) *Histogram matching* is performed to redistribute the intensity values of the input image for increasing contrast. iii) *Brightness specification* adjusts the image brightness values based on Hubbard's brightness specification [12]. The detailed description of each module is presented in the following subsections. Note that, Retinal images typically have a black border that needs to be eliminated. Within the STARE and DIARETDB0 datasets, many images show more border artifacts such as dark regions caused by uneven luminance, brighter areas caused by flash, and green or red timestamps on the border [11] [15]. Moreover, the macula area in some images is off-center. To overcome these artifacts and accurately obtain ROI, the input image data are captured with the rectangular area to crop the regions of interest around a macular area.

A. Specified Histogram Construction via Ordering Gap Adjustment Module

In OGABS algorithm, the input image from file image110.png is cropped by the black rectangular as shown in the Fig. 2, and Fig. 3 provides to demonstrate the operations. The specified histograms of each color channel has three sub-routines as the follows.

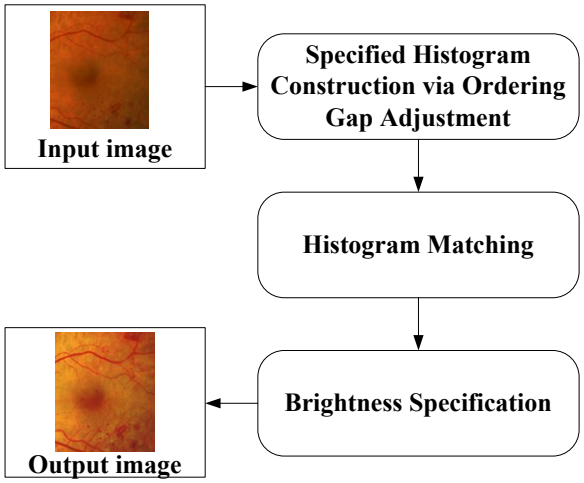

Fig. 1 The functional block diagram of the proposed method.

A.1. Histogram Segmentation

The pixel data in ROI are manipulated to creates histograms of each color channel and then to segment into three sub-histograms namely *left-tail*, *foremost* and *right-tail* sub-histograms as seen in Fig. 3 (a).

Given X_c be the color channel *c-th* of the input image, *X,* and *c* consists of R, G, and B channels. Let *x* be the intensity levels in X_c, with the range [0, L-1] where L denotes the maximum intensity values. The number of pixels in each intensity level, $H_c(x)$, is the histogram of X_c.

Four parameters in *c-th* color channel including $x_{s,c}$, $x_{l,c}$, $x_{r,c}$, and, $x_{e,c}$ as shown in Fig. 3 (a) are used to partition the intensity ranges of the histograms into $[x_{s,c}, x_{l,c} -1]$, $[x_{l,c}, x_{r,c}]$, and $[x_{r,c} +1, x_{e,c}]$. From the study in [4], they defined the image contrast by four times of the standard deviation values with the centroid at mean values. In our algorithm, these parameters are adapted to specify the brightness values as the follows.

$$x_{s,c} = 0, \tag{1}$$

$$x_{l,c} = \text{mean}(X_c) - (2 * \text{SD}(X_c)), \tag{2}$$

$$x_{r,c} = \text{mean}(X_c) + (2 * \text{SD}(X_c)), \tag{3}$$

$$x_{e,c} = \max_x (p_c(x) > 0). \tag{4}$$

Where mean and SD are the average and the standard deviation of intensity values, X_c, respectively. The maximum value, $x_{e,c}$ is formulated by probability of occurrence ($p_c(x)$ as seen in eq. (6)) at the maximum intensity that must be greater than zero. The histogram of the original green channel is shown in Fig. 3 (a), the four parameters are $x_{s,G} = 0$, $x_{l,G} = 40$, $x_{r,G} = 104$, and $x_{e,G} = 143$.

As shown in Fig. 3 (a), the four parameters are employed to segment the histogram, $H_c(x)$ of a color channel, *c*-th as denoted, $H_c[x_{s,c}\ x_{e,c}]$ into the three sub-histogram including the

left-tail (LT), foremost (FM) and right-tail (RT). The segmented histograms formulate by the following.

$$H_c[x_{s,c},x_{e,c}] = LT_c[x_{s,c},x_{l,c}-1]\cup FM_c[x_{l,c},x_{r,c}]\cup RT_c[x_{r,c}+1,x_{e,c}]. \quad (5)$$

The probability density function of an intensity level x, $p_c(x)$, is represented by:

$$p_c(x) = H_c(x)/(m\times n), \quad (6)$$

where the size of image is $m \times n$ pixels.

A.2. Histogram Ordering Gap Adjustment

In the color retinal images, retinal pigment epithelium (RPE) is a background, which can be displayed against AMD abnormality [12]. From the studied datasets, when uses frequency analysis by histogram, both the red and green channels have a highest frequency on the RPE background. Therefore, we select the background to adjust a distance or gap between the intensity values.

Fig. 2 The original image of image110.png.

The main purpose of this process is to adjust the gap between adjacent intensity values in order to improve the image contrast. Due to the left and right-tail sub-histograms easily introduced artifactual texture when the dynamic range is increased; thus, the dynamic range will be increased only for the foremost sub-histogram while the left and right-tail sub-histogram remains unchanged. The algorithm initials to compute the available spaces in the foremost sub-histogram for appending the gap between adjacent intensity in order to increase the dynamic range. The available spaces, s_c, can be specified by subtracting Hubbard's dynamic range specifications, *HD*, with the dynamic range of *FM*, *FD* as the follows:

$$s_c = HD_c - FD_c. \quad (7)$$

Where HD_c is defined to 128 (for c = {R, G}) following [12] and FD_c is the dynamic range of FM_c. For color retinal image, each channel, c, has its own characteristic resulting in different *FD* calculation. As the green channel typically provides more anatomical structure details and is considered to be more robust against noise compared to other channels, thus the *FD* of the green channel is calculated from $x_{r,G} - x_{l,G}$. In the case of Fig. 3 (a), the $FD_G = x_{r,G} - x_{l,G} = 104 - 40 = 64$. The available space, $s_G = 128 - 64 = 64$. From Eq. (7), the lower value of *FD* gives more available spaces s to increase the dynamic range. However the red channel, it is simply too bright or oversaturated when increasing the dynamic range; thus, the FD_R will be calculated from $x_{e,R} - x_{s,R}$. Finally, the blue channel contains almost no information and is usually distributed in a narrow interval [16], hence, the blue channel is translated only to the specified brightness in step II.C.

To determine the number of gaps that will be inserted between an adjacent intensity in the foremost sub-histogram, the gaps should be appropriated based on the values of the limiter function, $G(x)$, in order to make the output image meet the minimum requirement of human visual perception for the contrast change in each intensity value [17].

$$G(x)=\text{ROUND}(u\times[(x/127)-1]^2)+v. \quad (8)$$

$G(x)$ denotes the limiting gap of each intensity value, x. The parameter values were assigned $u = 3$ and $v = 3$ as introduced by Chiu and Ting [17] to control the levels of enhancement.

To select the number of bins for representing the background that could be used proportion between the number of available span spaces, s_c, in Eq. (7) and the limiting gap, $G(x)$, in Eq. (8). Thus, the bin numbers, q, could be estimated from:

$$q=\text{ROUND}(s_c / G(x)). \quad (9)$$

From our investigation, the intensity variable, x, in eq. (8) could be replaced with Hubbard's brightness specifications, {192, 96, 32} for red, green, and blue, respectively. From our example in Fig. 3 (a), x_G in Eq. (8) is replaced with 96, provides $G(x_G=96) = 3$; therefore, $q = 21$ which means that 21-bins of the intensity of the background are rearranged.

In rearranging process, the sub-histograms, FM_c, are ordered by descending as seen in Fig. 3 (b). 21 descending bins are selected to adjust gaps between bins equal to $G(x_G) = 3$, and assigning to new foremost sub-histogram, FM'_G, as shown in Fig. 3 (c).

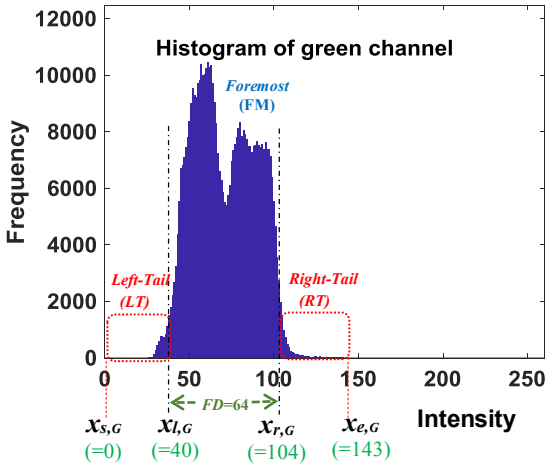

(a) Original image histogram and the labelled parameters

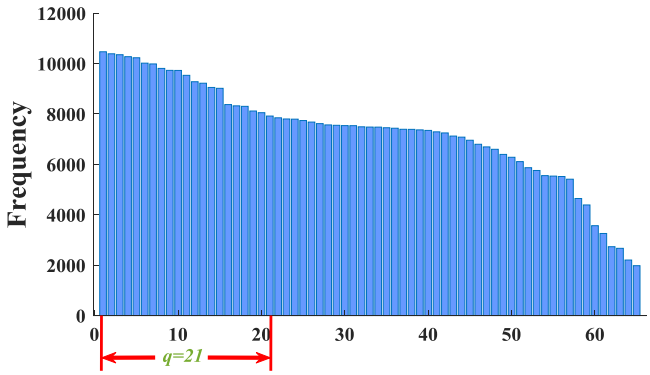

(b) The bin numbers, q

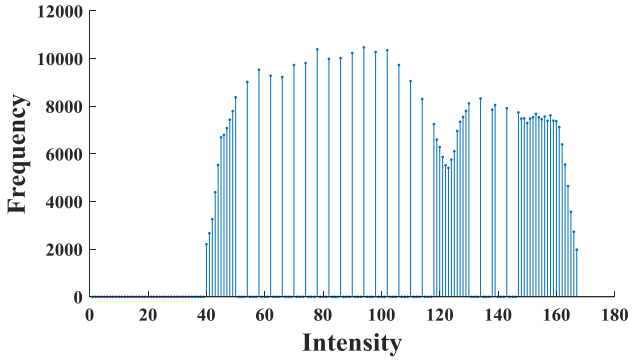

(c) FM'_G

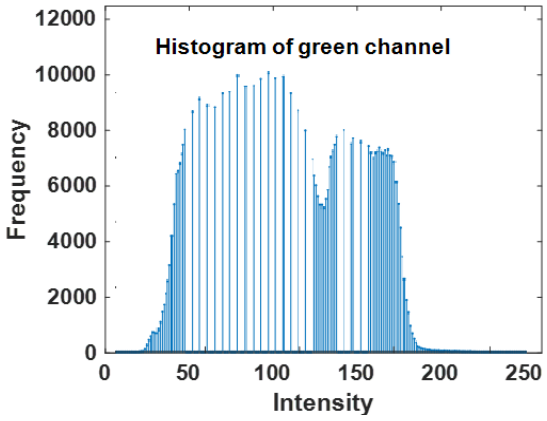

(d) H'_G

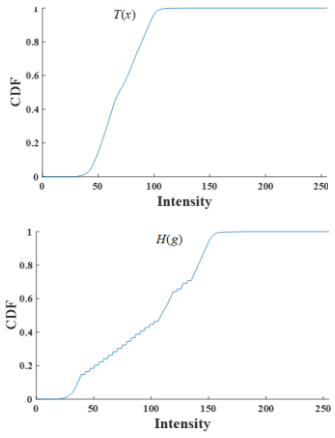

(e) CDF of original and enhanced image

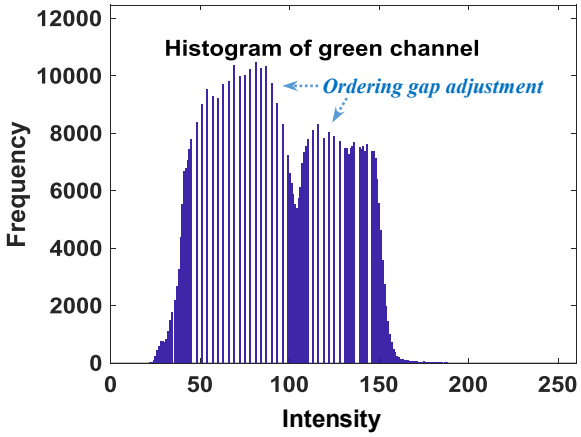

(f) Brightness specified histogram, g'_G

Fig. 3 Operation results of OGABS algorithm.

A.3. Specified Histogram Construction

The specified histogram, H'_c, can be obtained by recombining FM'_c from the process *A.2* with the left-tail sub-histogram (LT_c) and right-tail sub-histogram (RT_c) as the follows:

$$H'_c[x_{s,c},x_{e,c}] = LT_c[x_{s,c},x_{l,c}-1] \cup FM'_c[x_{l,c},x_{r',c}] \cup RT_c[x_{r',c}+1,x_{e,c}+(x_{r'}-x_r)] \quad (10)$$

The specified histogram of the green channel, H'_G, is illustrated in Fig. 3 (d).

In our experiment, the right-tail sub-histogram of some retinal images, especially for the STARE dataset, has a very long tail. This leads to out of range problem when $x_{e,c}+(x_{r'}-x_r)$ is outside the 8-bits range. In order to reduce pixel values

above 255, in this case, the right-tail sub-histogram, RT_c will be compressed within 255 by using shrink function [18] as:

$$\text{Shrink}(I(m,n))=S_{min}+\left(\frac{S_{max}-S_{min}}{I(m,n)_{max}-I(m,n)_{min}}\right)\bullet\left(I(m,n)-I(m,n)_{min}\right). \quad (11)$$

Where I is the intensity values of RT_c that need to be compressed. S_{min} and S_{max} are the desired minimum and maximum intensity levels which are set to $[x_{r',c}+1, 255]$. Those new intensity values are used to generate a compressed version of right-tail sub-histogram that did not exceed 255 levels.

B. Histogram Matching

The obtained specified histogram derived from *A.3* as shown in Fig. 3 (d) is used to perform histogram matching to redistribute the intensity values of the input image. More detailed information of histogram matching can be found in Gonzalez *et al*. [18].

Let $T(x)$ denotes the cumulative density function from PDF, $p_c(x)$, in Eq. (6); thus, $T(x)$ is defined by:

$$T(x)=\int_{-\infty}^{x} p_c(u)\,du, \quad (12)$$

where u is a dummy variable of integration.

The specified histogram, $p_g(g)$ can be reached by replacing the $H_c(x)$ in Eq. (6) by $H'_c(x)$ in Eq. (10). The CDF of specified histogram can be expressed in the form:

$$H(g)=\int_{-\infty}^{g} p_g(v)\,dv, \quad (13)$$

where v is a dummy variable of integration.

From Eq. (6) and (7), both $T(x)$ and $H(g)$ must be equal to unity as shown in Fig. 3 (e); hence, the output intensity level, g of the desired image becomes:

$$g_c=H^{-1}(T(x)), \quad (14)$$

where H^{-1} is an inverse transformation function which maps every intensity values in the input image to the desired output image.

C. Color Balance Improvement

Usually, the contrast enhanced images, g_c, from Eq. (14) have mean values deviated from the specified brightness vector, sb_c = [192, 96, 32]. To adjust the brightness and color balance following the color model of Hubbard *et al*., the color offset of the images, g_c, are adjusted by shifting the mean values of g_c to the specified brightness values, sb_c, as given by:

$$g'_c=g_c+(sb_c-\mu_c). \quad (15)$$

The histogram of g'_c is shown in Fig. 3 (f).

In Fig. 3, we showed only the operations of the green channel. The red channel could be operated as the same process with the green; except the blue channel have to operate only the Eq. (15). Fig. 4 illustrates the image result from our algorithm. For other results will be shown in the experimentations.

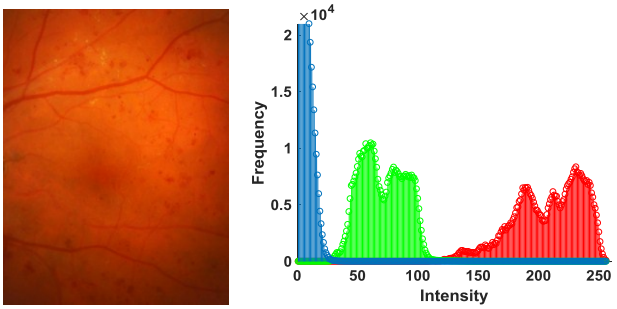

(a) The original and its histogram of image110.png

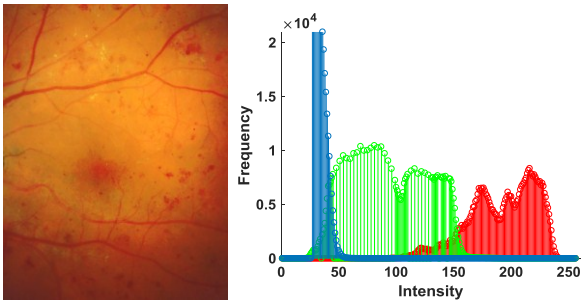

(b) The enhanced image with proposed method

Fig. 4 The original and enhanced image and its histogram

III. EXPERIMENTAL RESULTS

In the experimentation, our method is compared with the color retinal image enhancement based on luminosity and contrast adjustment (LCA) [9] and the method designed for AMD classification namely an automatic screening and grading of AMD from texture analysis of fundus image (ASG) [11]. Two datasets, STARE and DiaretDB0 are provided for evaluating the performance of the algorithms. The evaluation processes consist of showing proportion of unsatisfactory images before and after enhancement, objective assessment, and inspection of visual quality.

A. Percentage of unsatisfactory images before and after enhancement

Hubbard *et al.* classified the undesirable retinal image into four groups [12]: 1) oversaturation of red (if the pixel values $x_R \geq 240$ have the pixel number greater than 15%), 2) marked under illumination (the brightness value of red channel less than 96), 3) weak green or strong red (the brightness ratio, G/R < 0.40), and 4) excessive blue (the brightness ratio, B/R > 0.25). Due to the undesirable images are not easy to visual diagnosis the AMD abnormalities against the normal RPE background.

TABLE I: Percentage of unsatisfactory images before and after enhancement.

Undesirable Type	Dataset	Before	After
Oversaturation of Red Marked Under Illumination	STARE	53.13 %	0.19 %
	DiaretDB0	4.62 %	0 %
Weak Green/ Strong Red	DiaretDB0	56.92 %	0 %
Excessive Blue	STARE	37.50 %	0 %

From dataset investigation, STARE has oversaturated images where 53.13% and 37.50% of the images are found with an excessive blue channel. DiaretDB0 provides with weak green or strong red images 56.92%. Table I shows the percentage of undesirable images before and after processing by our method.

B. Image characteristics before and after enhancement

In our experimentations, the image characteristics are provided to evaluate the color retinal images which are specified by Hubbard *et al.* [12]. Table II summarizes the image characteristics compared between the original and our enhanced images. The image data consists of 32 images for STARE and 130 images for DiaretDB0. Both datasets were examined for their brightness, color balance ratios, and contrast which calculated from the standard deviation of intensity values in each color band. The second column is the image channels. The enhanced images by our method achieve the following target values. The average brightness (Mean ± SD) of red, green, and blue channels, for DiaretDB0 are 191.95 ± 0.29, 96.13 ± 1.7, and 32.01 ± 0.35, and for STARE are 191.85 ± 0.53, 97.49 ± 6.19, and 32.1 ± 0.30, respectively. The average ratios (Mean ± SD) of green-to-red and blue-to-red of DiaretDB0 are 0.5 ± 0.01 and 0.17 ± 0.00, and STARE are 0.51 ± 0.03 and 0.17 ± 0.00. Ranges in each color channel are illustrated in the form [Min - Max]. As provided with TABLE II, our method could adjust the intensity data in each color channel following the specifications of AMD reading center [12].

TABLE II: Image characteristics of DiaretDB0 and STARE datasets before and after enhancement.

Features	Channel	DiaretDB0		STARE	
		Original Image Mean ± SD [Min - Max]	Enhanced Image Mean ± SD [Min - Max]	Original Image Mean ± SD [Min - Max]	Enhanced Image Mean ± SD [Min - Max]
Brightness	Red	145.31 ± 33.71 [42.46 - 233.24]	191.95 ± 0.29 [191.27 - 192.48]	193.84 ± 38.40 [115.38 - 247.75]	191.85 ± 0.53 [190.05 - 192.49]
	Green	55.9 ± 14.81 [20.86 - 99.36]	96.13 ± 1.70 [95.51 - 114.27]	111.93 ± 32.59 [57.35 - 195.26]	97.49 ± 6.19 [95.51 - 127.82]
	Blue	9.63 ± 7.04 [0.12 – 33.00]	32.01 ± 0.35 [31.52 – 34.00]	47.17 ± 35.07 [2.78 - 186.89]	32.1 ± 0.30 [31.52 - 32.50]
Contrast	Red	22.55 ± 6.72 [9.44 - 48.22]	23.13 ± 5.48 [10.77 - 38.88]	32.13 ± 15.35 [7.52 - 62.68]	31.32 ± 12.77 [14.12 - 59.39]
	Green	11.30 ± 3.93 [4.89 - 24.52]	27.28 ± 4.89 [14.5 - 38.69]	22.47 ± 10.30 [8.97 - 44.19]	34.45 ± 4.98 [24.29 - 46.95]
	Blue	5.07 ± 2.29 [0.38 - 13.46]	4.95 ± 2.27 [0.38 - 13.46]	16.79 ± 7.73 [2.66 - 39.03]	15.4 ± 6.04 [2.66 - 27.29]
Color Balance	Green/Red	0.39 ± 0.06 [0.25 - 0.50]	0.5 ± 0.01 [0.5 - 0.59]	0.59 ± 0.18 [0.29 - 1.16]	0.51 ± 0.03 [0.5 - 0.67]
	Blue/Red	0.07 ± 0.05 [0.00 - 0.20]	0.17 ± 0.00 [0.16 - 0.18]	0.26 ± 0.22 [0.01 - 1.26]	0.17 ± 0.00 [0.16 - 0.17]

C. Objective Assessment

The proposed method is designed to improve the quality of image contrast, color balance, and naturalness. To evaluate the performance of our method, various quantitative metrics including global contrast factor (GCF) [19], measuring colorfulness ($M^{(3)}$) [20], and lightness order error (LOE) [21] are used to measure the image contrast, color, and naturalness preservation, respectively.

GCF [19] provides to assess image contrast at various resolution levels by creating a weighted average to get the global contrast factor. Since GCF was designed for measuring the grayscale images; however, in the color retinal images, we use only the green channel to evaluate the image contrast;

because, this channel contains informative details of the retinal structures [5].

$M^{(3)}$ [20] was formulated to metric colorfulness which fits the perceptual data collected from a psychophysical experiment and it has a simple expression based on the opponent color.

LOE [21] measures the lightness order error between the original and output image to assess the naturalness preservation. LOE could judge how well the enhancement method preserves the naturalness from the input image. The smaller the LOE values, the better the naturalness is preserved.

Table III shows the quantitative metric values, where each row is the enhancement method and each column is the quantitative metrics shown with average and standard deviation values (Mean ± SD) calculated for 32 STARE images and 130 DiaretDB0 images. From Table III, the proposed method yields the highest GCF (3.20±0.56) and $M^{(3)}$ (79.47±8.73). These highest scores imply that the proposed method performs better than both ASG and LCA methods for the case of improving contrast and colorfulness. For the naturalness, our method has the lowest scores (LOE = 4.04±10.16); therefore, the algorithm well preserves the naturalness and outperforms the ASG and LCA method.

TABLE III: Performance of various methods on DiaretDB0 and STARE datasets.

Method	Dataset	GCF	$M^{(3)}$	LOE
ASG	DiaretDB0	0.85±0.31	62.3±12.68	0.70±5.69
	STARE	1.08±0.52	80.51±18.16	13.84±30.69
	Both	0.92±0.37	70.42±17.12	8.75±18.68
LCA	DiaretDB0	2.32±0.55	56.82±14.96	649.24±193.26
	STARE	3.62±1.12	93.31±21.74	593.25±311.30
	Both	2.97±0.84	75.07±18.35	621.25±252.28
Proposed method	DiaretDB0	2.63±0.49	70.63±5.75	0.52±3.33
	STARE	3.77±0.62	88.30±11.71	7.56±16.99
	Both	3.20±0.56	79.47±8.73	4.04±10.16

D. Visual Assessment

From the quantitative evaluation, OGABS algorithm provides the good performance; however, only numerical outcomes do not confirm the visual diagnosis having good quality for detecting the AMD lesions. The enhanced images can be appreciated where the resultant image gives a pleasing natural appearance. Fig. 5 shows the output results from the DiaretDB0 dataset. The first column represents the original images. The next columns illustrate the image results of ASG, LCA, and OGABS methods. In this picture, all images have poor color and contrast, as seen from the last column our method could improve outperform ASG and LCA. Fig. 6 emphasizes on an abnormal lesion like hard/soft exudates, hemorrhages, and red small dots. The output images by employing ASG gives a little bit brighter in bright regions especially for drusen but the details of vessels are not easily seen; however, LCA method seems to generate dark color on the blood vessels and hemorrhage lesions. The proposed method produces a pleasing in visual appearance and maintains the color balance better than other methods.

Some retinal images from STARE dataset are also employed to assess our algorithm. In Fig. 7, the enhanced results by LCA could generated dark color areas and leading to obscure the anatomical structures of the images. The ASG method is able to improve the brighter yellow regions; however, the other areas are not easily observed especially in the vessel areas. OGABS provides natural color and high contrast. In Fig. 8, contained the small yellowish and hemorrhage regions, our enhanced results provide easy visible the lesions due to improved image contrast and color balance when compared to the original and output images from ASG and LCA methods.

In particularly, the proposed method cannot only enhance the contrast of anatomical details but can also produces a standard color of the AMD lesions such as the drusen always appears in yellow color and haemorrhage appears in red color. This will help novice ophthalmologists to easily detect drusen and haemorrhage for making decisions in diagnosis of dry and wet AMD.

As shown in Fig. 5 to 8 and supporting for TABLE I to III, our method could handle the different factors between FOV and the spatial resolutions. Although the retinal photographs from STARE are equipped with smaller the resolutions than the images from DiaretDB0; however, our enhanced results provide the highest contrast and color balance looking natural as the film photographs [5] [12]. For the other datasets such as DiaretDB1 [22] or Messidor [23], those datasets gave spatial resolutions not less than STARE; thus, OGABS could support them.

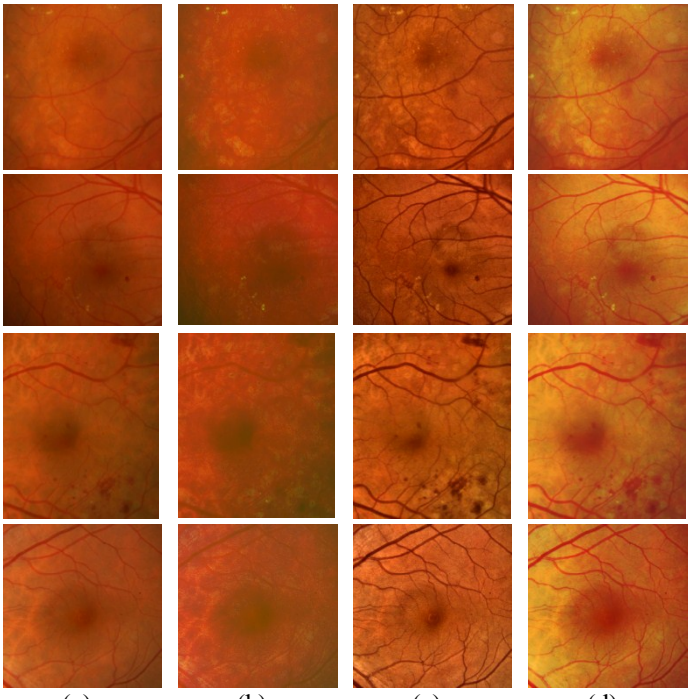

(a) (b) (c) (d)

Fig. 5 The results of different methods for the image image001.png, image005.png, image010.png, and image130.png from DiaretDB0.
(a) Original, (b) ASG, (c) LCA, and (d) OGABS.

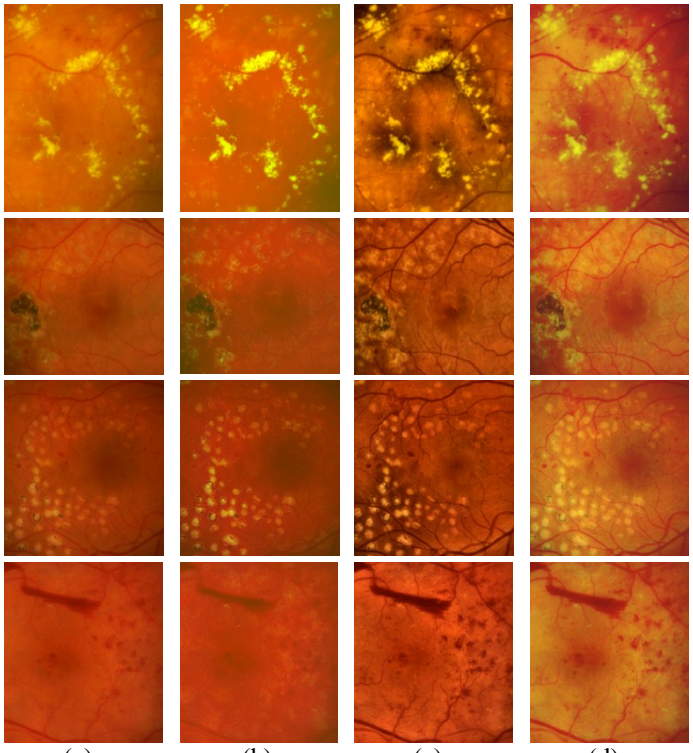

(a) (b) (c) (d)

Fig. 6 The results of different methods for the image image013.png, image040.png, image050.png, and image046.png from DiaretDB0.
(a) Original, (b) ASG, (c) LCA, and (d) OGABS.

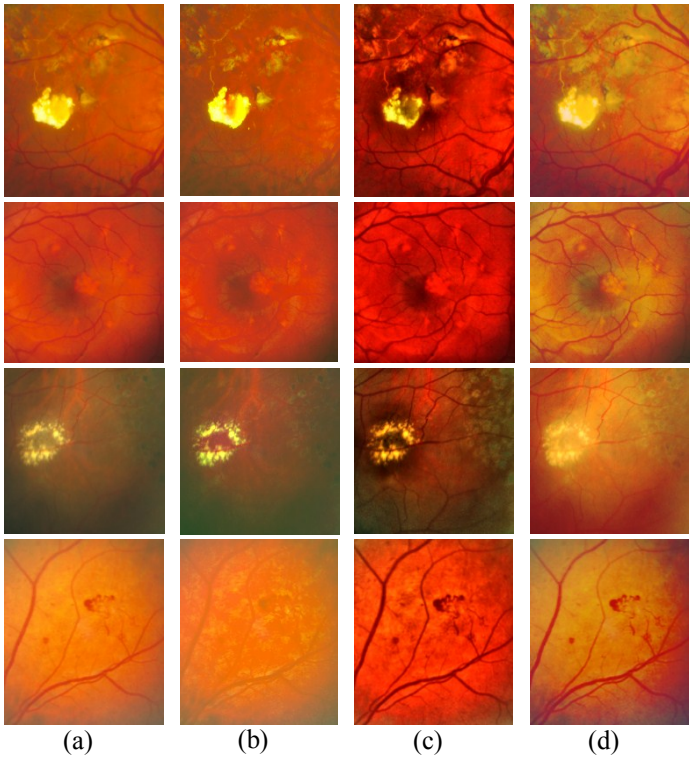

(a) (b) (c) (d)

Fig. 7 The results of different methods for the image im0052.png, im0102.png, im0316.png, and im0354.png from STARE.
(a) Original, (b) ASG, (c) LCA, and (d) OGABS.

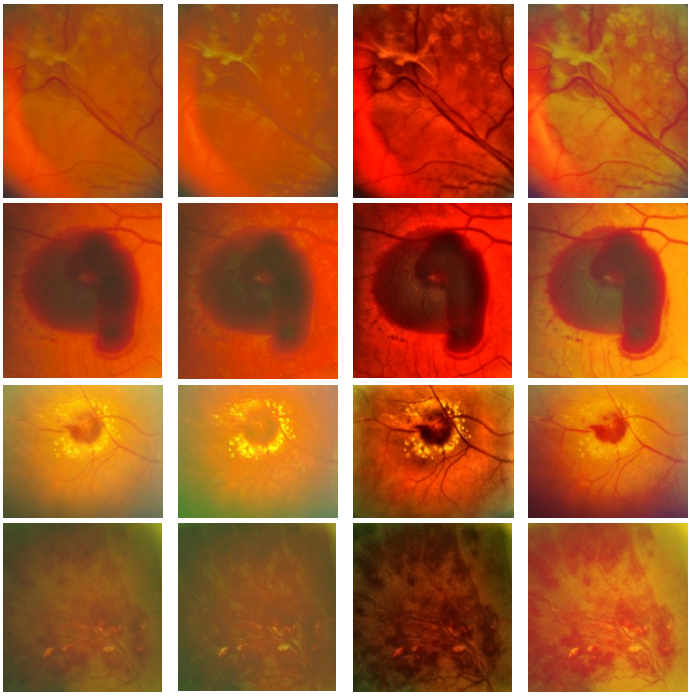

(a) (b) (c) (d)

Fig. 8 The results of different methods for the image im0356.png, im0357.png, im0359.png, and im0367.png from STARE
(a) Original, (b) ASG, (c) LCA, and (d) OGABS.

IV. CONCLUSIONS

In this paper, the color retinal image enhancement method was developed by employing the ordering gap adjustment and brightness specification named as OGABS algorithm. The algorithm adjusted contrast and color balance, and preserved naturalness of the color retinal images; because, the gap adjustment rearranged the RPE background to produce high contrast against AMD abnormalities; and when mapping the color data distribution to Hubbard's color model, the image results were provided with more naturalness leading to the impression of high quality photographs from film. Our method was tested on retinal images from the STARE and DiaretDB0 datasets. The proposed method achieved the contributions for improving the image quality as seen from the experimentation results that obtain the highest contrast, color balance, and natural looking than the other methods.

RERERENCES

[1] W. H. Organization, "World Health Organization," [Online]. Available: http://www.who.int/blindness/causes/priority/en/index7.html.

[2] W. L. Wong, X. Su, X. Li and C. M. G. Cheung, "Global prevalence of age-related macular degeneration and disease burden projection for 2020 and 2040: a systematic review and meta-analysis," *The Lancet Global Health,* vol. 2, no. 2, pp. 106-116, 2014.

[3] S. H. Rasta, M. E. Partovi, H. Seyedarabi and A. Javadzadeh, "A comparative study on preprocessing techniques in diabetic retinopathy retinal images: illumination correction and contrast enhancement," *Journal of Medical Signals and Sensors,* vol. 5, no. 1, pp. 40-48, 2015.

[4] E. Tsikata, I. Lains, J. Gil and M. Marques, "Automated brightness and contrast adjustment of color fundus photographs for the grading of age-related macular degeneration," *Translational Vision Science & Technology,* vol. 6, no. 2, pp. 3, 2017.

[5] L. D. Hubbard, "Digital color fundus image quality: the impact of tonal resolution," Spring/2009 Vol 31:1 p.15. [Online]. Available: http://www.opsweb.org/?page=crareference. [Accessed 16 June 2015].

[6] C. Wang and Z. Ye, "Brightness preserving histogram equalization with maximum entropy: a variational perspective," *IEEE Trans. Consum. Electron.,* vol. 51, no. 4, p. 1326–1334, 2005.

[7] H. Ibrahim and N. Kong, "Brightness preserving dynamic histogram equalization for image contrast enhancement," *IEEE Trans. Consum. Electron.,* vol. 53, pp. 1752–1758, 2007.

[8] D. Sheet, H. Garud, A. Suveer, M. Mahadevappa and J. Chatterjee, "Brightness preserving dynamic fuzzy histogram equalization," *IEEE Trans. Consum. Electron,* vol. 56, no. 4, pp. 2475-2480, 2010.

[9] Z. Mei, J. Kai, W. Shaoze, Y. Juan and Q. Dahong, "Color retinal image enhancement based on luminosity and contrast adjustment," *IEEE Rev. Biomed. Eng.,* no. 99, pp. 1-7, 2017.

[10] K. Zuiderveld, Contrast limited adaptive histogram equalization, San Diego: Academic press professional, pp.474-485, 1994.

[11] T. V. Phan, L. Seoud, H. Chakor and F. Cheriet, "Automatic screening and grading of age-related macular degeneration from texture analysis of fundus images," *Journal of Ophthalmology,* vol. 5893601, pp. 1-11, 2016.

[12] L. D. Hubbard, R. P. Danis, M. W. Neider, H. D. Thayer, H. D. Wabers, J. K. White, A. J. pugliese and m. F. Pugliese, "Brightness, contrast, and color balance of digital versus film retinal Images in the age-related eye disease study 2," *Journal of Investigative Ophthalmology & Visual Science,* vol. 49, no. 8, pp. 3269-3282, 2008.

[13] A. Hoover, V. Kouznetsova and M. Goldbaum, "Locationg blood vessels in retinal images by piecewise threshold probing of a matched filter response," *IEEE Trans. Med. Imag,* vol. 19, no. 3, pp. 203-210, 2000.

[14] T. Kauppi, V. Kalesnykiene, J. K. Kammarainen, L. Lensu, L. Sorri, H. Uusitalo and H. Kalviainen, "DIARETDB0 : Evaluation database and methodology for diabetic retinopathy algorithms," in *Technical report*, Lappeenranta, finland, 2006.

[15] S. Kankanahalli, P. M. Brlina, Y. Wolfson, D. E. Freund and N. M. Bressler, "Automated classification of severity of age-related macular degeneration from fundus photographs," *Invest Ophthalmos Vis Sci.,* vol. 54, no. 3, pp. 1789-1796, 2013.

[16] L. A. Hamid, A. E. Rafei, S. E. Ramly, G. Michelson and J. Hornegger, "Retinal image quality assessment based on image clarity and content," *J. Biomed. Opt.,* vol. 21, no. 9, pp. 096007, 2016.

[17] C. C. Chiu and C. C. Ting, "Contrast enhancement algorithm based on gap adjustment for histogram equalization," *Sensors,* vol. 16, no. 6, pp. 936 (1-18), 2016.

[18] C. R. Gonzalez and E. R. Woods, Digital image processing, 3rd edn., Pearson, 2009.

[19] K. Matkovic, L. Neumann, A. Neumann, T. Psik and W. Purgathofer, "Global contrast factor - a new approach to image contrast," in *Computational Aesthetics in Graphics, Visualization and Imaging*, Girona, Spain, pp. 159-167, 2005.

[20] D. Hasler and S. Susstrunk, "Measuring colorfulness in natural images," *Proc. SPIE,* vol. 5007, pp. 87-95, 2003.

[21] S. Wang, J. Zheng, H. Hu and B. Li, "Naturalness preserved enhancement algorithm for non-uniform illumination images," *Trans. Image Process.,* vol. 22, no. 9, pp. 60-70, 2013.

[22] K. Tomi, K. Valentina, K. J. Kristian, L. Lasse and S. Liris, "Diaretdb1 diabetic retinopathy database and evaluation protocol," in *in Proc. of the British Machine Vision Conference*, University of Warwick, UK, pp.252-261, 2007.

[23] E. Decenciere, J. C. Klein and X. Zhang, "Feedback on a publicly distributed image database: The Messidor database," *Image Anal Stereol ,* vol. 33, pp. 231-234, 2014.